Proceedings Ninth Workshop Geothermal Reservoir Engineering
Stanford University, Stanford, California, December 1983
SGP-TR-74

THE GENERATING CAPACITY OF THE HEBER GEOTHERMAL FIELD, CALIFORNIA

M. J. Lippmann and G. S. Bodvarsson

Earth Sciences Division
Lawrence Berkeley Laboratory
University of California
Berkeley, CA 94720

ABSTRACT

Using numerical simulation techniques and the radial model developed for the study of the natural state of the Heber field (Lippmann and Bodvarsson, 1983b), the response of this geothermal system to exploitation is analyzed. In this study the generation rate in the field is allowed to build up over a period of 10 years; after that, 30 years of constant power production is assumed. Full (100%) injection of the spent brines is considered, the fluids being injected 2250 m ("near injection") or 4250 m ("far injection") from the center of the system. The study shows that a maximum of 6000 kg/s (equivalent to approximately 300 MW_e) of fluids may be produced for the near injection case, but only 3000 kg/s (equivalent to approximately 150 MW_e) for the far injection case. The results indicate that the possible extraction rates (generating capacity) generally are limited by the pressure drop in the reservoir. The average temperature of the produced fluids will decline 10-18°C over the 40-year period.

INTRODUCTION

Construction of the first power plant at the Heber geothermal field (Fig. 1) began in June 1983. It will be a 45 MW_e (net) binary plant and is scheduled to come on-line in 1985. The construction of a second facility, a 47 MW_e (net) dual-flash power plant, will begin in early 1984; its completion is also targeted for 1985. Further development at Heber might follow. Chevron Geothermal Co., the operator of the field, estimates that the Heber anomaly can support a power generation of 500 MW_e for at least 30 years (Salveson and Cooper, 1981; California Division of Oil and Gas, 1983).

The objective of this paper is to evaluate the generating capacity of the Heber system under different production-injection scenarios. The response of the field to exploitation is calculated using a numerical simulator that computes heat and mass transport in geothermal systems. The initial temperature and pressure distributions and the boundary conditions assumed in these calculations correspond to those determined by the natural state model of Heber developed previously (Lippmann and Bodvarsson, 1983b).

PREVIOUS WORK

The only published modeling study on the exploitation of the Heber reservoir is that by Tansev and Wasserman (1978). They use a three-dimensional, single-phase (liquid) non-isothermal simulator. Their model of the geothermal reservoir covers a 30.3 km^2 area and consists of two main zones: Zone 1, from 2000 to 4000 ft (600 to 1200 m) depth, and Zone 2, from 4000 to 6000 ft (1200 to 1800 m) depth. Zone 1 is subdivided into 15 horizontal sand and shale layers, and Zone 2, into 13 layers. The model is further divided into 8 areal pies, each consisting of 15 rows.

Tansev and Wasserman (1978) assume that: (1) the sand and shale layers are continuous, homogeneous and isotropic, (2) the initial temperatures vary only as a function of the radial coordinate, and do not vary vertically in a given zone, (3) the regional ground water movement is negligible, (4) no heat (or mass) recharge occur from the underburden (below 1800 m), and (5) (in most cases studied) no cross flow exists between the pies into which the model is divided. No data is given on the thermal and hydraulic properties assigned to the different layers.

Fluids are assumed to be produced from both zones (between 600 and 1800 m depth) to sustain a constant 200 MW_e total generating capacity. Hot fluids are extracted near the axis of the system and the spent brine is reinjected near its periphery (the exact locations are not given). The initial total fluid production rate is 4.56 m^3/s, but as the temperature of the produced fluids decreases the production rate increases. Some of the conclusions reached by Tansev and Wasserman (1978) are: (1) both zones show a 16.7°C temperature decline over a thirty year production period, (2) the Heber system between 600 and 1800 m (Zones 1 and 2) alone can support 250 MW_e power production, and (3) in general, the generating capacity of Heber will be restricted mainly by the pressure drop rather than by the temperature decline (a temperature of 160°C for the power plant is assumed as a economic cutoff point).

AVAILABLE DATA

Only information on the reservoir development plan will be reviewed since the published data on the subsurface characteristics of the Heber system have been summarized elsewhere (Lippmann and Bodvarsson, 1983b).

According to Tansev and Wasserman (1978), Chevron plans to develop a nearly circular 30.3 km^2 area with each plant increment representing a pie-shaped segment. Salveson and Cooper (1981) indicate that the "wells will be directionally drilled for production from surface islands into the high temperature part of the thermal anomaly. Bottom hole locations will be evenly distributed in a circular pattern having a radius of about 600 m.

The power plants will be located near the producing islands to minimize heat loss during transit of the hot brine. Cooled brine will be piped from the power plants to injection islands on the periphery of the field. There, 2.4-4.0 km from the center of the anomaly, the spent brine will be reinjected through directionally drilled wells to the present position of the 129°C isotherm."

For the production depths assumed by Tansev and Wasserman (1978) -- 600 to 1800 m -- 2.28 m^3/s of fluid will initially be required to generate 100 MW_e. For a fluid density of 900 kg/m^3, this would correspond to about 2050 kg/s. Lacey and Nelson (1982; Fig. 2) state that 995 kg/s of geothermal fluids are needed for the 45 MW_e (net) binary plant. For the 47 MW_e (net) dual flash plant De Haven (1982) mentions a rate of about 1020 kg/s. In other words, about 1000 kg/s of fluid will be required to generate 50 MW of electrical power.

One hundred percent of the fluids produced from the reservoir will be reinjected; some makeup waters from surface sources will be required. For the 45 MW_e (net) plant the temperature of the injected fluids will be 72.2°C (Lacy and Nelson, 1982; Fig. 2). No other reference indicating the temperature of the injected brines was found in the literature.

METHODOLOGY

LBL's three-dimensional simulator PT (Bodvarsson, 1982) is used to compute the heat and mass flow through the system in response to different assumed development plans. The change of reservoir pressures and the average temperature of the produced fluids are the main parameters used to establish the feasibility of the fluid production-injection schemes considered in this study.

DESCRIPTION OF THE MODEL

The model used in the simulations is almost identical to the one applied for studying the natural state of the Heber system (Lippmann and Bodvarsson, 1983b). The radially symmetric model presents five zones of different material properties (Fig. 2).

Boundary conditions. The outer boundary of the model, 10 km from the axis, is assumed to be open to heat and mass flow and have constant temperatures and pressures. The temperatures at the outer boundary are assumed to increase linearly with depth with a gradient of 50°C/km. The pressures used at the outer boundary are hydrostatic for the assumed temperature distribution.

The top boundary is considered open only to heat flow; it is kept at a constant temperature of 22°C, which corresponds to the mean annual temperature in the area. Most of the bottom boundary, at 4950 m depth, is assumed to be closed to fluid flow and to have a constant temperature of 269.5°C, computed from the assumed geothermal gradient and surface temperature. However, in a circular area around the axis of the system, 1000-m in radius, the lower boundary is left open to fluid flow. This area has a constant temperature and pressure of 244.5°C and 456.7 bars, respectively. Under natural state conditions these parameters result in a mass recharge through the axial lower area of the system. This is equal to that of the 14.6 kg/s convective heat source inferred to exist at the bottom of the upflow zone at the Heber field (Lippmann and Bodvarsson, 1983b). During the simulation of the exploitation of the system, this rate of recharge will increase with time as the reservoir pressure in the upflow zone decreases. Thus, the modeling of the upflow zone using a constant pressure boundary is an optimistic assumption. The different treatment of the inner lower boundary (constant pressure as opposed to constant flow rate) is the only disparity between the models used to simulate the behavior of the system before and during exploitation.

Initial conditions. The initial temperature and pressure conditions used in simulating the exploitation of the field correspond to those of the natural state model discussed by Lippmann and Bodvarsson (1983b). Figure 3 shows the initial distribution of temperatures (because of symmetry only half of the cross section is given).

Rock properties. The reservoir system is divided into 5 zones with different rock properties, primarily different permeability values (Table 1). Zones 1 and 2 are 550 m thick and represent the caprock. Zone 3, which corresponds to a cylinder of 1000 m radius, is the hot water upflow zone. Zones 4 and 5 correspond to the outer regions of the field.

The most important reservoir parameters controlling the distribution of temperature and pressure in the system under natural (steady-state) conditions are the permeability and thermal conductivity. These are determined for the different zones by modeling Heber in its pre-exploitation state (Lippmann and Bodvarsson, 1983b). To our knowledge no values have been published on the porosity of the Heber reservoir. In our work we use porosities which are in the range of those found in other geothermal fields of the Salton Trough (Riney et al., 1980; Lippmann and Bodvarsson, 1983a).

Fluid properties. The geothermal fluid is assumed to be pure water; its density, viscosity and compressibility are allowed to vary with temperature and pressure. The specific heat of the fluid is kept constant (4,200 kJ/kg); its thermal expansivity is neglected.

Produced zones. Fluids are produced from the 1000-m radius upflow zone (Zone 3). In two of the four cases studied (Cases 1 and 2) production is uniformly distributed between depths of 650 m and 2950 m. This production scheme is similar to the one discussed by Salveson and Cooper (1981).

In Cases 3 and 4, the production is assumed to be restricted to deeper formations (the 1950-2950 m depth interval) facing the higher permeability Zone 5 (Fig. 2).

Production rates. The main objective of this study is to find out what extraction rates (i.e., generating capacity) are possible at Heber for different injection scenarios. It is assumed that during a

10-year period the installed generating capacity at Heber increases linearly with time, from zero MW_e at t = 0 to a maximum value at 10 years. From then on, the electrical power generation remains constant at the maximum level.

The simulations are carried out until boiling is observed in some part of the system (this always occurs in the shallow reservoir region near the axis), or to 100 years, whichever occurs first. When boiling occurs, the reservoir pressure at the upper part of the produced zone (at 750 m depth in Cases 1 and 2) generally drops about 40 bars, a drawdown considered to be excessive for a pumped system like that planned at Heber. Based on the published data noted above, it is assumed that 1000 kg/s of geothermal fluids are required to generate 50 MW_e.

Injected zones. One hundred percent of the fluids extracted from the reservoir are reinjected. At each depth interval the same mass of fluid is injected as is produced. Several radial distances from the axis of the system are considered for reinjection (Fig. 4). Two extreme situations are discussed here.

Near Injection: Uniform injection into a circular region extending between 2000 and 2500 m from the axis of the system (Cases 1 and 3);

Far Injection: Uniform injection into a circular region extending between 4000 and 4500 m from the axis (Cases 2 and 4).

These two extremes bound the radial distances indicated by Salveson and Cooper (1981) for the location of the injected zones; i.e., 2.4-4.0 km.

Temperature of the injected brine. Following Lacy and Nelson (1982; Fig. 2) it is assumed that the injected fluid has a temperature of 72.2°C.

RESULTS

Four reservoir development plans (cases) are discussed (see Table 2). In the first two cases fluid is produced from between 650 and 2950 m depths; the plan is similar to that described by Salveson and Cooper (1981). Cases 3 and 4 study the effect of producing (and injecting) all fluid from a deeper 1000-m thick interval located adjacent to (or in) the higher permeability Zone 5.

The computed changes in reservoir pressures and average temperature of the produced fluids for the four cases are given in Figures 5 to 15. For Case 1, the temperature, pressure and mass flow distribution in the system are shown in Figures 16 to 18. The production characteristics after 40 years of development for all cases studies are summarized in Table 3.

Reservoir Pressures

The shape of the pressure versus time graphs for the production nodes reflects the assumed field development plan. Between 0 and 10 years the total production rate increases linearly with time, from zero to a maximum rate at 10 years. This causes large pressure declines at early times. Later on, pressures tend to stabilize due to constant extraction rates and injection effects.

In Cases 1 and 2 the drawdown in the upper part of the produced interval (Fig. 5 and 8) is much larger than that in the lower part (Fig. 6 and 9). This is mainly due to the limited fluid recharge to the shallower zones of the production region. In the upper part of the production zone, the lateral recharge is limited because of the relatively low horizontal permeability (10 md) of Zone 4. In comparison, for the lower part of the production zone, the horizontal permeability of the neighboring Zone 5 is 115 md. The effect of the permeability distribution on the pressure drop in the reservoir is evident in Figure 17 which shows pressure contours for Case 1 after 40 years of exploitation. The effect of permeability contrast is also evident in the magnitude of the recharge to the different regions of the production zone, as illustrated in Figure 18; the length of the arrows is proportional to the mass flow rate.

In order to circumvent the effect of the lower permeability Zone 4, in Cases 3 and 4 the production and injection was restricted to the 1950-2950 m depth interval (Table 2). In these cases, even though the fluid extraction rate per unit volume of production zone has more than doubled with respect to Cases 1 and 2, the drawdown has been reduced considerably. No boiling occurs in the system even when the production rate is as high as 10,000 kg/s (Fig. 12 and 14).

The reservoir pressure support of the reinjection operations is clearly evident when one compares, e.g., the 4000 kg/s examples, for Cases 1 and 2 (Fig. 5 and 8, and 6 and 9). The closer to the production zone injection takes place, the greater is the pressure support. However, if fluids are injected too close to the production region, detrimental decreases in the temperature of the produced fluids occur (see below).

The pressures in the injection nodes located in Zone 4 are illustrated in Figure 11 (for Cases 1 and 2). There is a rapid rise in pressure as the injection (and production) rate increases during the first 10 years. From then on, as the rate is kept constant, the pressure stabilizes (Case 1) or even slowly decreases (Case 2). On the other hand, the pressure in the injection nodes located in the higher permeability zone (Zone 5) only changes slightly with time. For example, in Case 4 (far injecton) the total pressure rise after 40 years of injection at a rate of 10,000 kg/s is 3.5 bars.

Average Production Temperature

The temperatures reported here are the average temperatures of the produced fluids at the reservoir level; to obtain the temperature of the fluids at the inlet to the power plant one must consider the heat losses in the wellbore and also those in the surface hot water transmission pipes.

With production uniformly distributed over the 1000-m radius cylinder the initial average temperature of the produced fluids (weighted by mass) is 178.7°C for Cases 1 and 2, and 177.8°C for Cases

3 and 4. Because of the characteristic mushroom shape of the isotherms in the reservoir (Fig. 3), these average initial temperatures would be a few degrees higher if production is increased towards the axis of the system, and correspondingly reduced in the outer regions of the production cylinder. The changes in average fluid production temperatures with time for the different cases are given in Figures 7, 10, 13 and 15. The temperature of the produced fluids decreases significantly faster in Cases 1 and 3 (near injection) than in Cases 2 and 4 (far injection), because of the smaller distance between injection and production areas.

In Cases 3 and 4 the higher mobility of the injected fluids results in high overall temperature drops due to the larger permeability of Zone 5 and higher production/injection rates per unit volume. For equal total rates the temperature reductions are far greater than in Cases 1 and 2 (see Fig. 13 and 15). The higher mobility of the injected fluids in Zone 5 relative to that for Zone 4 is reflected, for Case 1 by the shape of the isotherms after 40 years of exploitation (Fig. 16), especially that of the 120°C isotherm.

The temperature of the produced fluids is not significantly affected if the temperature of the injected fluids is increased slightly (e.g., 100°C instead of 72.2°C). For example, in Case 1 (6000 kg/s), the average temperature after 40 years only increases from 163.6 to 163.9°C. However, because 100°C fluids have significantly lower viscosity than 72.2°C fluids, injection of higher temperature fluids is preferential for pressure support. In the example discussed above, the 100°C injection increases the "longevity" of the system from about 58 to about 70 years (Table 4).

"Longevity" of the System

The "longevity" of the system, considered here to correspond to the time boiling occurs somewhere in the system (excessive pressure drops), is given in Table 4 for the different cases studied. Based upon this criterion, and a minimum acceptable 40-year period, the results show that for Cases 1 and 2 the system cannot be produced at rates greater than 6000 and 3000 kg/s, respectively.

In Cases 3 and 4 the fluid extraction rate could reach, and possibly exceed, 10,000 kg/s (equivalent to about 500 MW_e). But, in these two cases the temperature reduction of the produced fluids, and not the drop in reservoir pressure, controls the maximum allowable fluid production rate. If one uses an economic temperature limit of 160°C for the power plant as indicated by Tansev and Wasserman (1978), and neglects any heat losses during transport in wellbore and surface pipes (i.e., temperature of the fluids at the reservoir equal to that at the power plant inlet), the maximum allowable production rate for a 40-year period is less than 6000 kg/s for Case 3 and slightly below 3000 kg/s for Case 4.

CONCLUSIONS

If one assumes a 40-year lifetime for the project, with 10 years to build up to the total electrical generating capacity and 30 years of maximum constant electrical power output, the results obtained show that (Table 3):

(1) For injection between 2000 and 2500 m from the axis of the system (near injection) a maximum production rate of 6000 kg/s (about 300 MW_e) is possible. However, it should be stressed that in Case 1, after 40 years of exploitation, the total pressure drop in the upper part of the produced region is 35.9 bars, and the average temperature of the produced fluids (at reservoir level) will have declined about 15°C, to about 164°C. For Case 3, the maximum possible mass extraction rate is below 6000 kg/s; for that rate after 40 years the production temperature would drop about 34°C, to about 144°C.

(2) For injection between 4000 and 4500 m (far injection) the maximum feasible production rate is 3000 kg/s (about 150 MW_e). In Case 2, after 40 years, the maximum drawdown in the reservoir (at r = 100 m, z = -750 m) is approximately 30 bars and the average temperature of production fluids 170°C. In Case 4, the pressure drop in the reservoir, at r = 100 m, z = -2700 m, is 12.0 bars and the temperature of the produced fluids will have dropped about 18°C, to about 159°C.

ACKNOWLEDGEMENTS

We thank our colleagues C. Doughty and J. Wang for reviewing the manuscript, as well as P. Fuller and C. Doughty for generating the computer plots used in the paper. This work was supported by the Assistant Secretary for Conservation and Renewable Energy, Office of Renewable Technology, Division of Geothermal and Hydropower Technologies of the U.S. Department of Energy under Contract No. DE-AC03-76SF00098.

DISCLAIMER

"This paper was prepared as an account of work sponsored by an agency of the United States Government. Neither the United States Government nor any agency thereof, nor any of their employees, makes any warranty, express or implied, or assumes any legal liability or responsibility for the accuracy, completeness, or usefulness of any information, apparatus, product, or process disclosed, or represents that its use would not infringe privately owned rights. Reference herein to any specific commercial product, process, or service by trade name, trademark, manufacturer, or otherwise, does not necessarily constitute or imply its endorsement, recommendation, or favoring by the United States Government or any agency thereof. The views and opinions of authors expressed herein do no necessarily state or reflect those of the United States Government of any agency thereof."

REFERENCES

Bodvarsson, G.S., 1982. Mathematical modeling of the behavior of geothermal systems under exploitation (Ph.D. thesis). Lawrence Berkeley Laboratory, report LBL-13937, 353 p.

California Division of Oil and Gas, 1983. Chevron, Dravo, may be partners in Heber dual flash project. Geothermal Hot Line, v. 13, No. 1, p. 7-8.

De Haven, N.J., 1982. Heber geothermal project. Geothermal Resources Council Trans., v. 6, p. 339-341.

Elders, W.A., J.R. Hoagland, E.R. Olson, S.D. McDowell, and P. Collier, 1978. A comprehensive study of samples from geothermal reservoirs. Riverside, Calif., Univ. of Calif. report UCR/IGPP-78/26, 264p.

Lacy, R.G. and T.T. Nelson, 1982. Heber binary project--Binary cycle geothermal demonstration power plant. Proc. Sixth Annual Geothermal Conference and Workshop, Electric Power Research Institute report EPRI AP-2760, p. 5-1 to 5-7.

Lippmann, M.J. and G.S. Bodvarsson, 1983a. Numerical studies of the heat and mass transport in the Cerro Prieto geothermal field, Mexico. Water Resour. Res., v. 19, p. 753-767.

Lippmann, M.J. and G.S. Bodvarsson, 1983b. A modeling study of the natural state of the Heber geothermal system, California. Geothermal Resources Council, Trans., v. 7, p. 441-447.

Riney, T.D., J.W. Pritchett, and L.F. Price, 1980. Integrated model of the shallow and deep hydrothermal systems in the East Mesa area, Imperial Valley, California. La Jolla, Calif., S-Cubed report SSS-R-80-4362, 116 p.

Salveson, J.O., and A.M. Cooper, 1981. Exploration and development of the Heber geothermal field, Imperial Valley, California. Proc. 1981 New Zealand Geothermal Workshop, p. 3-6.

Tansev, E.O., and M.L. Wasserman, 1978. Modeling the Heber geothermal reservoir. Geothermal Resources Council Trans., v. 2, p. 645-648.

Table 1. Rock properties used in the model.

Zone	Porosity	Horizontal Permeability (md)	Vertical Permeability (md)	Conductivity Rock-water Mixture (W/m°C)	Density (kg/m^3)
1	.30	5	0.5	1.088	2650
2	.30	5	0.05	1.088	2650
3	.23	125	12.5	2.000	2650
4	.25	10	0.1	2.000	2650
5	.23	115	11.5	2.000	2650

Note. Rock compressibility and thermal expansion are neglected.

Table 2. Reservoir development plans studied for the Heber field.

Case	Production/Injection depth intervals (m)	Average radial distance to injecton zones (m)
1	650 - 2950	2250
2	650 - 2950	4250
3	1950 - 2950	2250
4	1950 - 2950	4250

Note. In all cases fluid is produced from a 1000-m radius axial cylinder.

Table 3. Production characteristics after 40 years.

Fluid Production Rate (kg/s)	Reservoir* Pressure (bars)	ΔP^* (bars)	Average Temperature of Produced Fluids (°C)	$\Delta\overline{T}$ (°C)
		Case 1		
4000	55.5	-23.1	168.0	-10.7
5000	49.3	-29.4	165.8	-12.9
6000	42.8	-35.9	163.6	-15.1
		Case 2		
2000	59.1	-19.6	172.7	-6.0
3000	49.1	-29.6	170.1	-8.6
		Case 3		
6000	234.6	-19.7	144.1	-33.6
10,000	217.4	-37.0	126.8	-51.0
		Case 4		
3000	242.4	-12.0	159.2	-18.5
10,000	212.7	-41.7	146.0	-31.8

Note. *: For Cases 1 and 2 reservoir pressures correspond to the production node at r = 100 m and z = -750 m; for Cases 3 and 4, to the node at r = 100 m and z = -2700 m.

Table 4. "Longevity" of the System.[1]

Fluid Production Rate (kg/s)	Generating Capacity (MW_e)	Boiling in the system occurs after:
	Case 1	
4000	~200	>100 yrs
5000	~250	>100 yrs
6000	~300	~58 yrs (~70 yrs)[2]
7000	~350	~25 yrs
	Case 2	
2000	~100	>100 yrs
3000	~150	>100 yrs
4000	~200	~12.2 yrs
	Case 3	
6000	~300	>100 yrs[3]
10,000	~500	>100 yrs[3]
	Case 4	
3000	~150	>100 yrs[3]
10,000	~500	>100 yrs[3]

Notes. (1): See text for definition. (2): Injection of 100°C water.
(3): Based on pressure considerations only.

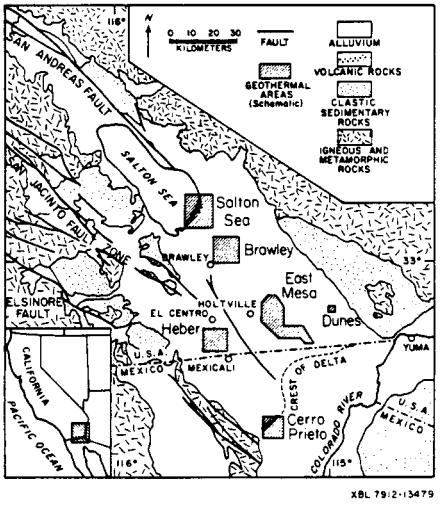

Figure 1. Location of geothermal areas in the Salton Trough (from Elders et al., 1978).

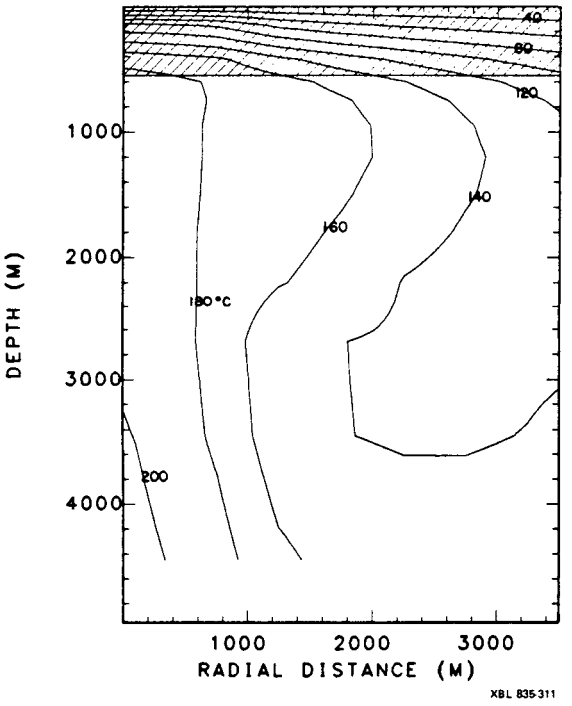

Figure 3. Initial distribution of temperatures in the system. Hatched layer represents the caprock (from Lippmann and Bodvarsson, 1983b).

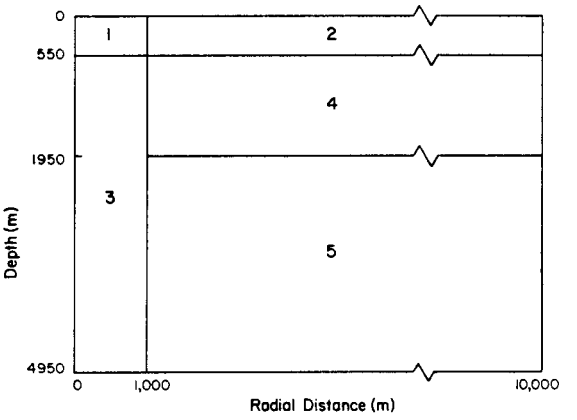

Figure 2. Different zones used in the model.

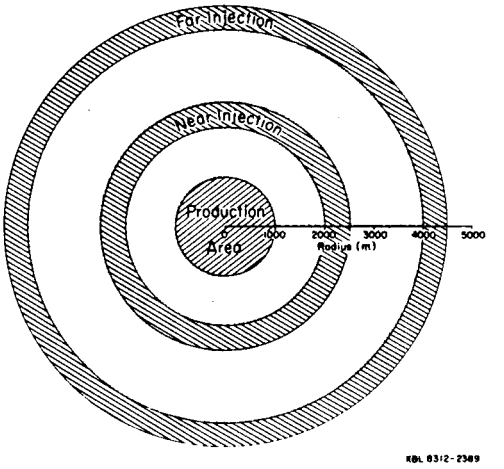

Figure 4. Plan view of the production/injection model used for Heber.

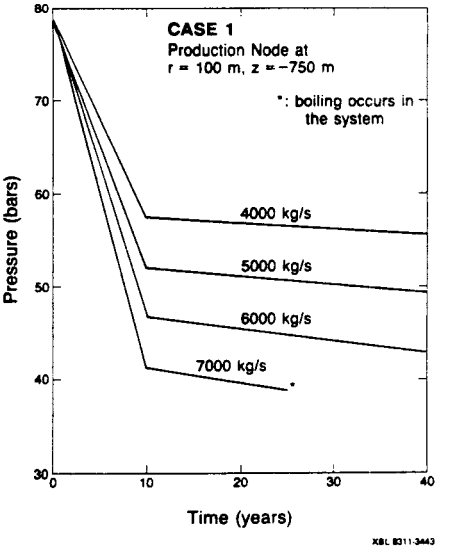

Figure 5. Case 1. Pressure in production node at r = 100 m, z = -750 m.

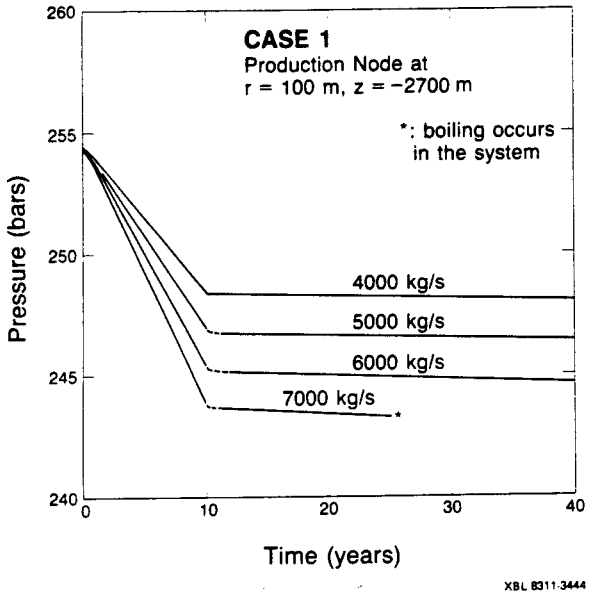

Figure 6. Case 1. Pressure in production node at r = 100 m, z = -2700 m.

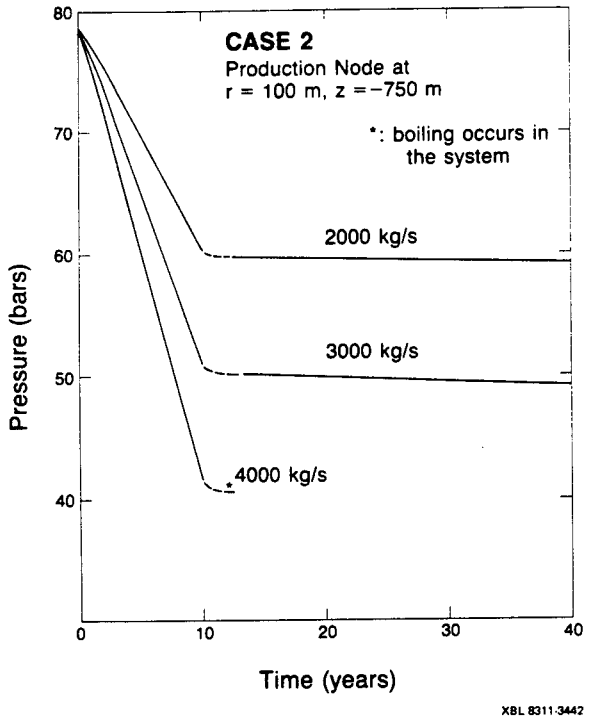

Figure 8. Case 2. Pressure in production node at r = 100 m, z = -750 m.

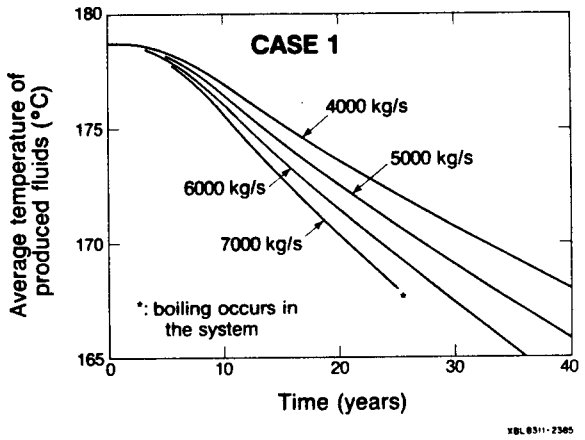

Figure 7. Case 1. Average temperature of produced fluids.

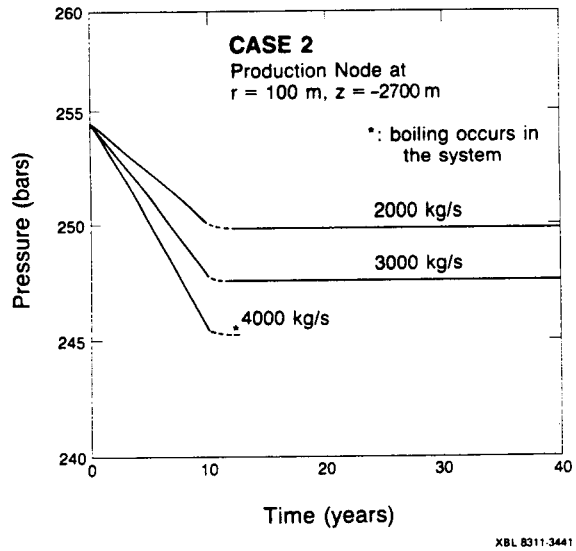

Figure 9. Case 2. Pressure in production node at r = 100 m, z = -2700 m.

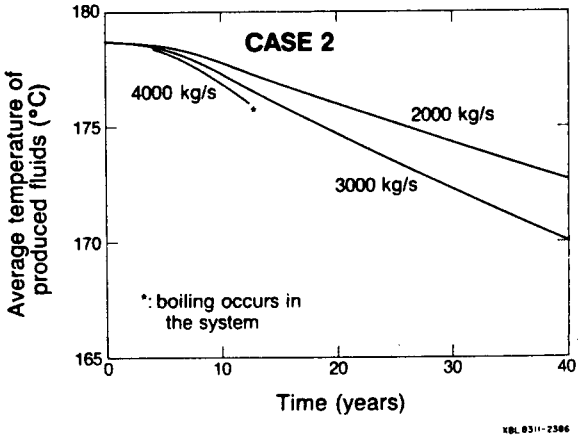

Figure 10. Case 2. Average temperature of produced fluids.

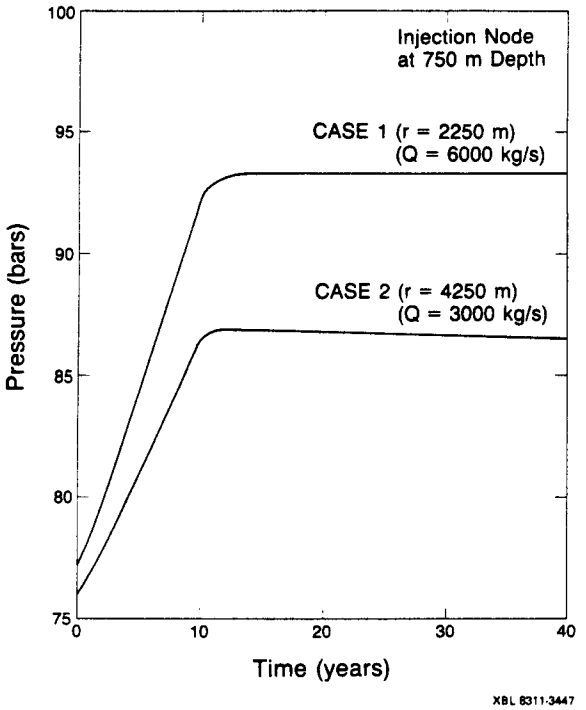

Figure 11. Cases 1 and 2. Pressure in injection node at 750 m depth.

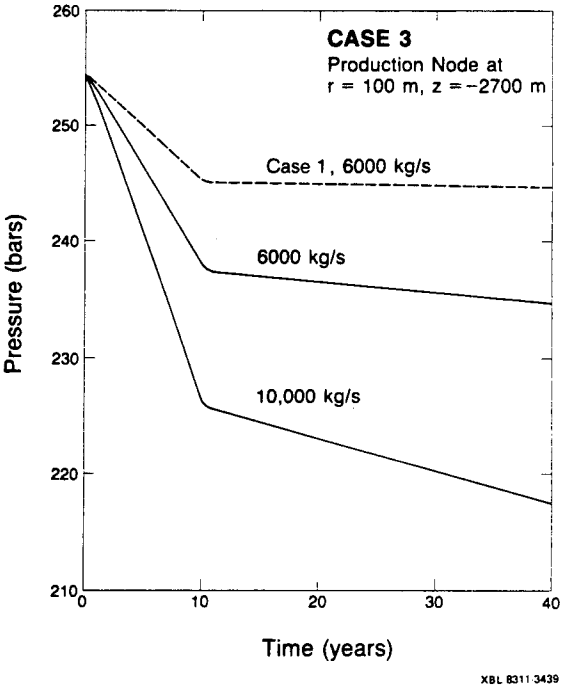

Figure 12. Case 3. Pressure in production node at r = 100 m, z = -2700 m.

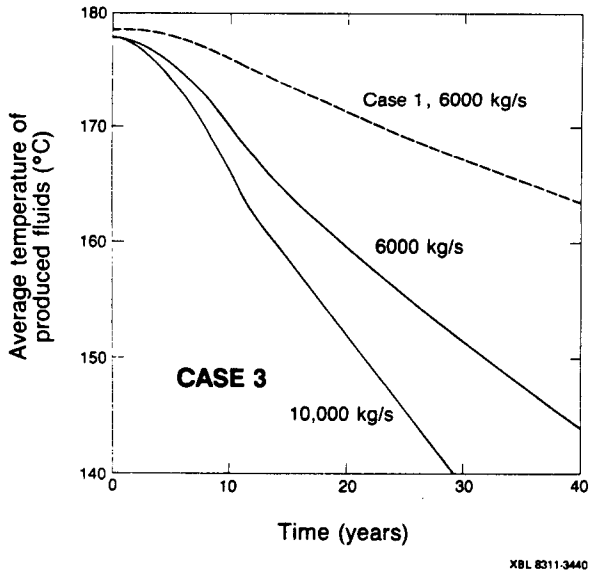

Figure 13. Case 3. Average temperature of produced fluids.

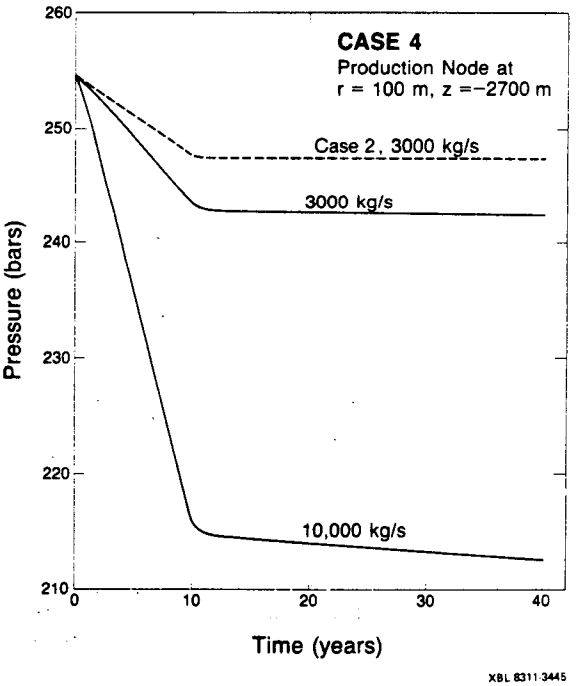

Figure 14. Case 4. Pressure in production node at r = 100 m, z = -2700 m.

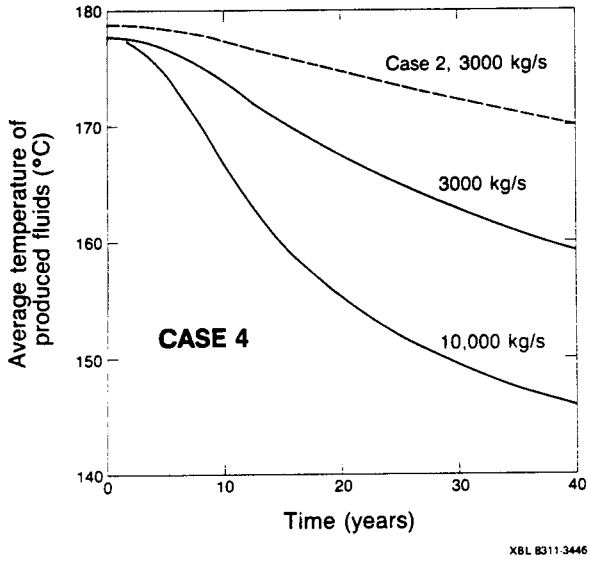

Figure 15. Case 4. Average temperature of produced fluids.

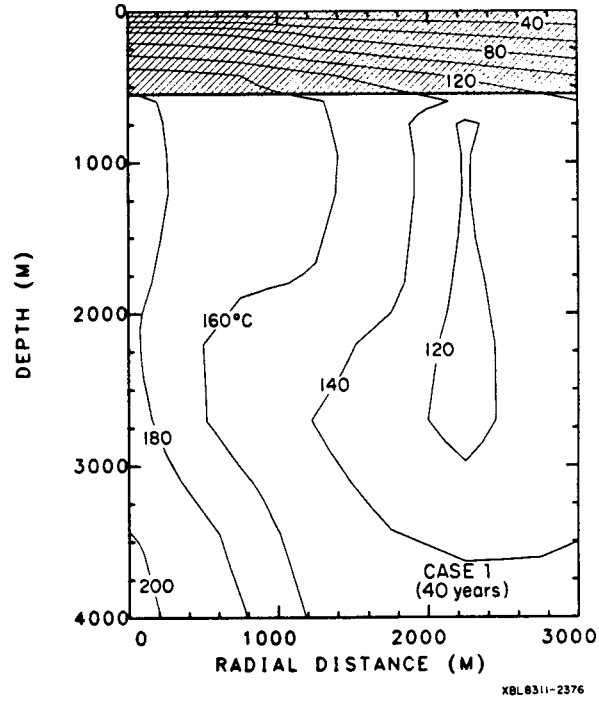

Figure 16. Case 1. Computed temperature distribution in the system after 40 years of exploitation. Hatched region represents the caprock.

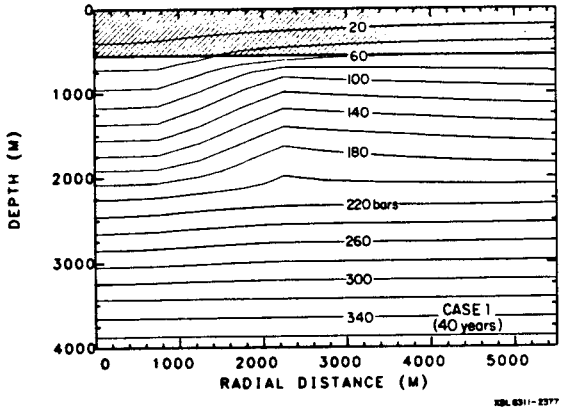

Figure 17. Case 1. Computed pressure distribution in the system after 40 years of exploitation. Hatched region represents the caprock.

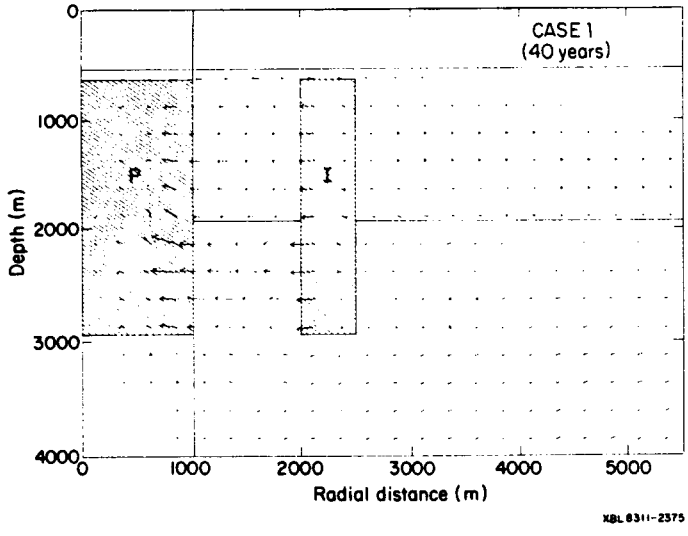

Figure 18. Case 1. Computed mass-flow pattern in the system after 40 years of exploitation. Length of arrows is scaled with respect to the largest mass flow rate. Lines delimit the different zones in the model. The hatched region represents the production (P) and injection (I) regions.